

An Optimal Power Control Algorithm for STDMA MAC Protocols in Multi-hop Wireless Networks

Siqian Cui, Homayoun Yousefi'zadeh, *Sr. Member IEEE* and Xuemai Gu, *Member, IEEE*.

Abstract—Multi-hop Spatial Time Division Multiple Access (STDMA) medium access control (MAC) protocols constitute an important building block of wireless networks. There are not many practical power control algorithms that can optimally trade off power consumption against transmission rates with a reasonable computational complexity. In this paper, we introduce an energy efficient distributed power control algorithm for STDMA MAC protocols. The motivation for this study is two fold, namely, maximizing the spatial reuse of the system resources and maximizing power efficiency. We develop a mathematical formulation for maximizing spatial reuse and power efficiency under discrete SINR and rate constraints. After proving that power is a convex function of data rates in our problem, we demonstrate that our problem in simultaneous transmission environments can be reduced to a Linear Programming (LP) problem. Then, we solve this LP problem using Dynamic Programming (DP). Finally, based on our proposed solution, we propose a low complexity Optimal Power Control (OPC) algorithm which can be generically embedded within any existing STDMA MAC protocol. Through analytical and experimental studies, we show that our power control algorithm can not only significantly improve the throughput, power consumption, and delay performance of STDMA MAC protocols compared to their baseline alternatives, but also outperform existing STDMA algorithms.

Index Terms—STDMA, optimal power control, rate adaptive, Linear Programming, Dynamic Programming.

I. INTRODUCTION

DESIGNING power and data rate strategies is one of the most important considerations in the design of wireless systems, since they directly affect the Quality of Service (QoS) offered to the users and the energy consumption of the system [1], [2]. Due to the limitation of the spectrum resources, exploiting effective MAC protocols for improving spatial channel reuse, i.e., increasing the number of concurrent transmission, is of high importance. Recently, a number of algorithms have been proposed that aim at combining power assignment and data rate adaptation in different kinds of multiple access wireless networks [3]–[7]. While these works have offered significant achievements in this important research topic, to date there are only a small number of energy efficient power control STDMA MAC algorithms that can practically trade off the assignment of power against the allocation of rate. Accordingly, the primary motivation of this work is to exploit

a high energy efficiency yet low complexity power control algorithm for multi-hop STDMA networks.

Embedding power control algorithms within MAC protocols has become more and more popular in the past decade. Theoretical studies have shown that proper use of power control algorithms in wireless MAC protocols can improve aggregate channel utilization by up to a factor of $O(\rho)$ where ρ is the density of nodes in the target region [8]–[11]. The use of power control algorithms in MAC protocols was originally proposed in the context of channelized cellular networks where power control algorithms were implemented in a centralized way, i.e., base stations centrally controlled channel and power assignments of all users [12], [13]. Later, the authors of [14]–[19] proposed distributed iterative power control algorithms for cellular systems and analyzed the corresponding convergence results. In order to improve the convergence characteristics of the distributed power control algorithms, the authors of [19] incorporated the notions of utility and cost in the context of a non-cooperative game theory problem. As evidenced by the works of [20]–[31], power control has also been explored as one of the key design aspects of the MAC protocols proposed for multi-hop wireless networks. The authors of [20] introduced a Power Control-based Multiple Access (PCMA) protocol which was limited to a class of Carrier Sense Multiple Access with Collision Avoidance (CSMA/CA) protocols of the IEEE 802.11 standard. They showed a factor of two improvement in aggregate channel utilization for PCMA compared to IEEE 802.11 protocol standard. In [21], a power-rate control scheme was developed for CSMA/CA wireless ad hoc networks capable of increasing the network throughput by finding near-optimal values of space-time per bit values. The authors of [24] introduced a contention-based multiple access protocol for STDMA multi-hop wireless networks based on making successful transmissions depending on a set of signal-to-interference-and-noise ratio (SINR) constraints. They proposed a solution with exponential complexity to a convex optimization problem of maximizing simultaneous transmissions with minimum average power in every time slot under universal SINR constraints. The authors of [25] solved the same problem as that of [24] by mapping it to a channelized cellular system problem and using the results already available. From among the list of relevant literature articles, we are most interested in the series of articles [28]–[31] from the same group of authors. In [28], the authors prove that minimizing the schedule length and corresponding transmit powers while meeting receiving SINR requirements is an NP-complete problem. They mathematically formulate this problem as a Mixed-Integer Linear Programming (MILP)

S. Cui is a PhD candidate at the Harbin Institute of Technology. In 2014, he was a Visiting Scholar at the University of California, Irvine (e-mail: siqian0303@gmail.com). H. Yousefi'zadeh is with the Center for Pervasive Communications and Computing at UC, Irvine (e-mail: hyousefi@uci.edu). X. Gu is with the Harbin Institute of Technology (e-mail: guxuemai@hit.edu.cn).

problem. Further more, they provide a heuristic algorithm to solve the problem using graph-coloring methods. The solutions of their MILP provide important benchmarks for the evaluation of heuristic scheduling algorithms in small scale multi-hop wireless networks. However, the complexity of their solution is still exponential. Building on the work of [28], [29] and [30] propose a new mathematical programming model and two centralized slot assignment algorithms for minimizing the schedule length in adaptive power and adaptive rate ways. Similar to the algorithm of [28], the proposed algorithms are centralized and can be solved in complexity orders of $\mathcal{O}(s^3m^2L^2)$ and $\mathcal{O}(s^3m + sL)$ where s is the spatial reuse factor of the network, m is the number of available data rates, and L is the number of links being scheduled. In order to offer lower complexity solution alternatives to the problems of [29] and [30], the authors of [31] present a distributive heuristic algorithm called Distributive Power control Rate adaptation Link scheduling (DPRL) algorithm. DPRL schedules multiple transmissions iteratively in a given time slot based on the highest $SINR$ value within the two-hop neighborhood not interfering with existing transmissions. As a greedy algorithm, DPRL has a complexity of $\mathcal{O}(m + (L/s)^2)$. While the complexity of this distributive heuristic algorithm is significantly reduced compared to its centralized counter parts, the powers assigned to the scheduled links are not optimized. In most instances, no more than two simultaneous transmissions can be found in a two-hop neighborhood. The most important shortcoming of the algorithms is the fact that the schedules are all static becoming invalid when nodes join or leave the network within the scheduled policy.

In this research, we propose a high energy efficiency power control algorithm that can be used to identify permissible simultaneous transmissions under SINR and rate constraints within the assigned time slot to a slot owner. We formulate our optimization problem first. Then, we investigate an approximated mathematical relationship between data rates and power levels within successful simultaneous transmissions. Based on our investigation, we introduce an equivalent LP problem and solve the problem using DP. Consequently, we propose a practical power control algorithm to which we refer as Optimal Power Control (OPC) algorithm. We evaluate performance by augmenting Dynamic Time Slot Assignment (DTSA) algorithm [32] and Unifying Slot Assignment Protocol Multiple Access (USAP) [33] protocols with our proposed algorithm. We also compare our algorithmic results with those of the algorithm proposed in [31]. The results show that our power control algorithm can not only significantly improve the throughput performance of STDMA MAC protocols while reducing the corresponding power consumptions, but also outperform DPRL.

The main contributions of this research are as follow. First, we develop a new mathematical formulation for maximizing spatial reuse and maximizing power efficiency in STDMA multi-hop wireless networks under discrete SINR thresholds constrains. Second, we investigate the approximated relationship between powers and data rates in simultaneous transmission environments. The latter provides us with a new perspective in allowing MAC protocols to support simultaneous

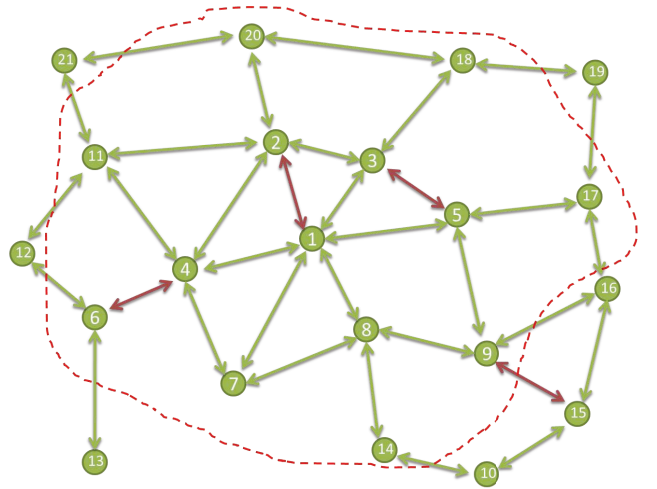


Fig. 1. The local contention area of Node 1 representing a typical network node.

transmissions in STDMA wireless networks. Third, we present a dynamic programming method to solve the resulting linear programming problems. Fourth, we propose a power efficient and low complexity optimal power control algorithm. Finally, we evaluate power consumption, throughput, and delay performance of our proposed algorithm by augmenting two existing protocols and comparing those with a previously proposed STDMA alternative. The rest of this paper is organized as follows. In Section II, we provide the system model. In Section III, we formulate the optimization problem. In Section IV, we present our power control algorithm and circumstances under which our algorithm is optimal. Simulation results and the corresponding analysis are provided in Section V. Conclusions are drawn in Section VI.

II. ANALYTICAL MODEL

In this section, we briefly introduce the underlying assumptions and associated notations that appear in this paper. The work of this paper is conducted in the context of STDMA and assuming the existence of time slot assignment strategies guaranteeing no two nodes within a two-hop neighborhood are assigned to the same time slot. Under the assumption of working with variable data rates, the range of one hop is defined as the transmission distance under the highest power in the lowest data rate. We use the concept of Local Contention Area (LCA) to represent a node's two-hop neighborhood and assume that the effective collision domain of a node is limited to its LCA [34]. However and similar to the approach of [31] and many other papers, we leave some "power margin" at the receivers to mitigate interference from nodes that are more than two hops away. From the stand point of practicality, we note that the use of LCA limits node discovery traffic to the local level as each node only concerns itself with knowing about its two-hop neighbors as oppose to the full set of network nodes. For illustration purposes, consider the topology of node 1's LCA as shown in Fig.1 and that the current slot is assigned to Node 1.

All nodes are assumed to be half-duplex and equipped with omnidirectional antennas. Each node generates fixed

length control and data packets in the process of every communication. We assume the communication link does not change during one time slot. We also assume data rates that can be selected by every node belong to the discrete set $\{r_1, r_2, \dots, r_m\}$ with $r_1 < r_2 < \dots < r_m$. Taking the size and weight limitations of the nodes into account, we assume that the maximum power available to each node is P_{max} .

Our algorithm will be executed at the beginning of each time slot. We assume that at the beginning of a time slot, transmitter i of an active link l_i^j has B_i^j packets to transmit to receiver j of the link. A successful transmission on a wireless link from node i to j can be established when the condition below is satisfied.

$$\frac{P_i^j G_i^j}{\sum I_k^j + N_j} \geq \gamma(r_i^j), \quad i \neq j \neq k \quad (1)$$

In the inequality above, r_i^j and P_i^j are the data rates from node i to node j and corresponding power used by the sending node i , respectively. N_j represents the thermal noise on receiver j , $\sum I_k^j$ is the interference caused by other simultaneous transmissions, and $\gamma(r_i^j)$ is the pre-specified SINR threshold which depends on factors such as data rate, acceptable Bit Error Rate (BER), and so on [31]. Further, the SINR threshold is only a function of r_i^j within a slot duration as other factors are assumed to be constant. Finally, G_i^j represents the path loss from node i to node j calculated according to the radio propagation model given below.

$$G_i^j = \frac{1}{d^\theta} \quad (2)$$

In the equation above, θ is the path loss exponent ranging from 2 when in the line of sight free space environment to 4 when in indoor environment [35]. We further note that the effects of wireless channel such as fading and shadowing can be captured by the expressions of Packet Error Rate (PER) if so desired [36], [37]. In this paper, we consider limited mobility scenarios of operation allowing to work with a fixed gain matrix in each execution period of our operational algorithm. We further assume that ACKs and control messages received by each node from its LCA neighbors contain the geographical GPS coordinates of the transmitting node [38]. We use the GPS coordinates for distance estimation as needed by our power control algorithm in section IV.

III. PROBLEM FORMULATION

In this section, we first formulate the problem that we want to solve with desired objectives and constraints. We then prove that this problem can be fully described using linear functions only. Consequently, we introduce an equivalent linear programming representation of the problem.

Our goal is to design a localized power and rate control algorithm which can be embedded within STDMA protocols to achieve the following objectives: (i) maximize the number of simultaneous transmissions in a given time slot, i.e., maximize the spatial reuse of the whole system resources; (ii) specify the set of powers and data rates of all of simultaneous transmissions in a power efficient manner; (iii) offer a low time complexity approach to apply our proposed algorithm. From

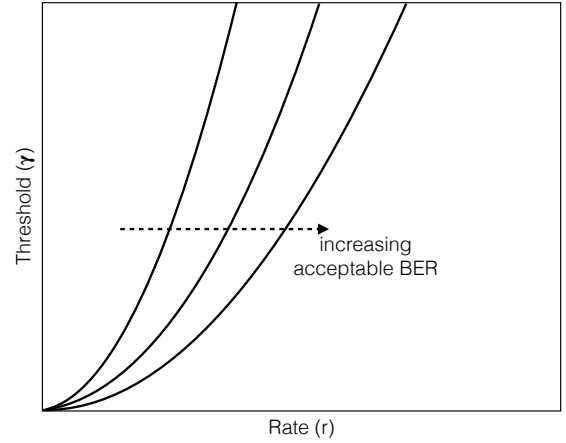


Fig. 2. Illustrations of Threshold (γ) as a function of Rate (r) and BER under a fixed channel state.

among the three objectives above, meeting objective (ii) is the main goal, i.e., achieving objective (i) and (iii) depends on the realization of objective (ii). Objective (ii) can be realized by solving the following optimization problem.

$$\begin{aligned} \max_{r_i^j, P_i^j} & \frac{\sum r_i^j}{\sum P_i^j} \\ \text{s.t.} & \begin{cases} r_i^j \in \{r_1, \dots, r_m\}, & r_1 < r_2 < \dots < r_m \\ 0 \leq P_i^j \leq P_{max} \\ r_{ith}^j \leq r_i^j \leq r_m \\ \frac{P_i^j G_i^j}{\sum I_k^j + N_j} \geq \gamma(r_i^j), & i \neq j \neq k \end{cases} \quad (3) \end{aligned}$$

In the problem above, r_{ith}^j is the smallest data rate that needs to be assigned to l_i^j . This quantity is related to the QoS required by the link. In the following, we will exploit and utilize the relationship between the power and data rate values in simultaneous transmission scenarios in order to simplify the problem formulation.

For a single transmitter-receiver pair, the transmit power necessary for a certain data rate (service) requirement depends on the distance between the transmitter and the receiver, the channel characteristics, acceptable BER, and many other factors. While there is no simple mathematical function to capture the latter, a fundamental aspect of this relationship exhibited by most modulation-encoding schemes [40]–[42] is as follows. For a fixed bit error probability and channel state, the required transmission power for reliable communication is a convex function of the data rate. Accordingly, it is easy to know that for a single transmitter-receiver pair, the necessary SINR threshold at the receiver is a convex function of data rate. The latter is illustrated in Fig. 2. The relationships between transmit powers and data rates are much more complicated for successful simultaneous transmissions, but nonetheless the corresponding $\gamma(r_i^j)$ levels should be met at the intended receivers of all links. Based on (1), the transmission power of a link depends on both that link's own data rate requirement as well as the data rate requirements of all other simultaneous transmissions. To identify the exact relationship between these quantities, we express and prove the following two theorems.

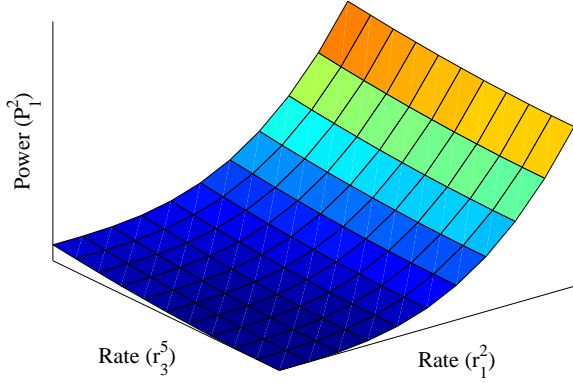


Fig. 3. An illustration of power P_1^2 as a function of rates r_1^2 and r_3^5 in simultaneous transmissions scenarios.

Theorem 1: For two simultaneous transmissions with links neither originated at the same transmitter nor converged at the same receiver and within the effective interference range, the power used by one link is a non-negative monotonically increasing convex function of the rate used by that link and the rate used by the other link.

See Appendix A for the proof.

Definition 1: We refer to the lowest data rate that can satisfy the QoS requirements of all links in an L simultaneous transmission scenario as Data Rate Threshold Point (DRTP).

Theorem 2: For L successful simultaneous transmissions, the highest power efficiency is obtained at the DRTP.

See Appendix B for the proof.

Theorem 2 implies that for simultaneous transmissions, transmitting packets at lower rates over longer durations is more energy efficient than at higher data rates over shorter durations. Many MAC protocols adopt the principle of “racing to sleep” [43] to reduce the probability of collisions and preclude simultaneous transmissions when simultaneous transmissions are in the interference region of the slot owner. Theorem 2 provides us with a new perspective in looking for a more appropriate treatment of simultaneous transmissions.

Assuming N represents the thermal noise signal at every receiver, applying Theorem 2 to the case of two simultaneous transmissions results in transforming the optimization problem

of (3) to the following LP problem.

$$\begin{aligned} \min \quad & \sum (P_1^2 + P_3^5) \\ \text{s.t.} \quad & \begin{cases} G_1^2 P_1^2 - G_3^2 \gamma(r_{1th}^2) P_3^5 \geq \gamma(r_{1th}^2) N \\ -G_1^5 \gamma(r_{3th}^5) P_1^2 + G_3^5 P_3^5 \geq \gamma(r_{3th}^5) N \\ r_{1th}^2, r_{3th}^5 \in \{r_1, r_2, \dots, r_m\}, \quad r_1 < r_2 < \dots < r_m \\ 0 \leq P_1^2, P_3^5 \leq P_{max} \end{cases} \end{aligned} \quad (4)$$

In the problem above, G_1^2 , G_3^5 , r_{1th}^2 , r_{3th}^5 and N are all constant. Consequently, the objective function and all of the constraints are linear functions. In the following section, we use dynamic programming to provide a low complexity solution to the problem.

IV. OPTIMAL POWER CONTROL

In this section, we first discuss how to utilize dynamic programming to identify the optimal power values used in simultaneous transmissions. Then, we devise a localized power control algorithm that enables the slot owners to support as many simultaneous transmissions as possible in a given time slot.

To illustrate how to formulate our problem as a dynamic programming solution, we define a few notations and variables first.

1) Stages and decisions: In our algorithm, we breakdown the procedure of specifying the powers used by n simultaneous transmissions into n steps and select the power of one link at each step. We call each step a “stage” and refer to the power selected in each stage as a “decision”. The decision in stage k is represented by x_k . In our problem, n stage procedures specify n optimal powers for n simultaneous transmission schedule should one exist. Using the definitions above and based on the results of Section III, we can restate our problem formulation for n simultaneous transmissions as follows.

$$\begin{aligned} \min_{x_i} \quad & (x_1 + x_2 + \dots + x_n) \\ \text{s.t.} \quad & \begin{cases} a_{1,1}x_1 + \dots + a_{1,k}x_k + \dots + a_{1,n}x_n \geq c_1 & \textcircled{1} \\ a_{2,1}x_1 + \dots + a_{2,k}x_k + \dots + a_{2,n}x_n \geq c_2 & \textcircled{2} \\ \dots & \\ a_{i,1}x_1 + \dots + a_{i,k}x_k + \dots + a_{i,n}x_n \geq c_i & \textcircled{i} \\ \dots & \\ a_{n,1}x_1 + \dots + a_{n,k}x_k + \dots + a_{n,n}x_n \geq c_n & \textcircled{n} \\ 0 \leq x_1, x_2, \dots, x_n \leq P_{max} & \end{cases} \end{aligned} \quad (5)$$

In the problem above, $a_{i,k}$ reflects the interference level of link k to link i , $a_{i,k} < 0$ when $i \neq k$, $a_{i,k} > 0$ when $i = k$, and $c_i = N\gamma(r_{ith}^j)$ where i and j are the sender and the receiver of link i , respectively. Take two links simultaneous transmissions formulated by (4) for example, $a_{1,1} = G_1^2$, $a_{1,2} = -G_3^2\gamma(r_{1th}^2)$, $a_{2,1} = -G_1^5\gamma(r_{3th}^5)$, $a_{2,2} = G_3^5$, $c_1 = N\gamma(r_{1th}^2)$, $c_2 = N\gamma(r_{3th}^5)$.

2) State at a stage: In our proposed method, associated with each stage of the optimization problem is the stage constraint with which the decision has to comply. We note that only the first k constraints are to be complied with at stage k . Thus at stage k ($k \leq n$), all factors except $a_{i,k}x_k$ in constraint i with $i \leq k$ are moved to the right hand side

and represented by R_{ik} . We define the right hand side of all constraints with $i \leq k$ together as the “state” S_k at stage k . Then, S_k is represented as shown below.

$$S_k = (R_{1,k}, \dots, R_{i,k}, \dots, R_{k,k}) \quad (6)$$

The constraints on x_k at stage k are $x_k \in S_k$ and are shown in detail as blow.

$$a_{i,k}x_k \geq R_{i,k}, \quad i \in \{1, \dots, k\} \quad (7)$$

Further, the state transition function is as follows.

$$R_{i,k} = R_{i,k-1} - a_{i,k-1}x_{k-1}, \quad i \in \{1, \dots, k\} \quad (8)$$

3) *Optimal objective function:* In our algorithm, we take the backward dynamic programming approach and define $f_k(S_k)$ to represent the minimum sum of the powers selected by stages k to n . Denoting x_k^* as the optimum decision of x_k , we define the optimal objective function as shown below.

$$\begin{cases} f_k(S_k) = \min_{x_k \in S_k} \{x_k + f_{k+1}(S_{k+1})\}, & k \leq n \\ f_{n+1}(S_{n+1}) = 0 \end{cases} \quad (9)$$

For $n = 2$, the optimal objective function is expressed as follows.

$$\begin{cases} f_k(S_k) = \min_{x_k \in S_k} \{x_k + f_{k+1}(S_{k+1})\}, & k \leq 2 \\ f_3(S_3) = 0 \end{cases} \quad (10)$$

When $k = 2$, we have

$$\begin{aligned} f_2(S_2) &= \min_{x_2 \in S_2} \{x_2 + f_3(S_3)\} \\ &= \min_{x_2 \in S_2} \{x_2\} \\ &= \min_{\frac{R_{2,2}}{a_{2,2}} \leq x_2 \leq \frac{-R_{1,2}}{|a_{1,2}|}} \{x_2\} \\ &= \min \left\{ \frac{R_{2,2}}{a_{2,2}}, \frac{-R_{1,2}}{|a_{1,2}|} \right\} \end{aligned} \quad (11)$$

When $k = 1$, we have

$$\begin{aligned} &f_1(S_1) \\ &= \min_{x_1 \in S_1} \{x_1 + f_2(S_2)\} \\ &= \min_{\frac{R_{1,1}}{a_{1,1}} \leq x_1 \leq P_{max}} \left\{ x_1 + \min \left(\frac{R_{2,2}}{a_{2,2}}, \frac{-R_{1,2}}{|a_{1,2}|} \right) \right\} \\ &= \min_{\frac{R_{1,1}}{a_{1,1}} \leq x_1 \leq P_{max}} \left\{ x_1 + \min \left(\frac{R_{2,1} - a_{2,1}x_1}{a_{2,2}}, \frac{a_{1,1}x_1 - R_{1,1}}{|a_{1,2}|} \right) \right\} \\ &= \min_{\frac{N\gamma(r_{1th}^2)}{G_1^2} \leq x_1 \leq P_{max}} \left\{ x_1 + \min \left(\frac{N\gamma(r_{3th}^5) + G_1^5\gamma(r_{3th}^5)x_1}{G_3^5}, \frac{G_1^2x_1 - N\gamma(r_{1th}^2)}{G_3^2\gamma(r_{1th}^2)} \right) \right\} \end{aligned} \quad (12)$$

We observe that the value of (12) decreases with a decrease in the value of x_1 . From a mathematical point of view only, the minimal value of (12) is reached at $x_1 = \frac{N\gamma(r_{1th}^2)}{G_1^2}$, i.e., the power selected by the slot owner can support its own transmission only. Obviously, this is not the value of x_1 that we seek. What we want is the value of x_1 under which two links can transmit simultaneously. Hence, the selection of the

value of x_1 has to allow for selecting at least one value that can support the transmission over link l_3^5 .

$$\min \left(\frac{N\gamma(r_{3th}^5) + G_1^5\gamma(r_{3th}^5)x_1}{G_3^5}, \frac{G_1^2x_1 - N\gamma(r_{1th}^2)}{G_3^2\gamma(r_{1th}^2)} \right) \quad (13)$$

Obviously, the value of (13) decreases as the value of x_1 decreases and the smallest value is achieved when the upper bound is equal to the lower bound.

$$\frac{N\gamma(r_{3th}^5) + G_1^5\gamma(r_{3th}^5)x_1}{G_3^5} = \frac{G_1^2x_1 - N\gamma(r_{1th}^2)}{G_3^2\gamma(r_{1th}^2)} \quad (14)$$

Then, we get the optimal x_1 as shown below.

$$x_1^* = \frac{G_3^5N\gamma(r_{1th}^2) + G_1^2N\gamma(r_{1th}^2)\gamma(r_{3th}^5)}{G_1^2G_3^5 - G_3^2G_1^5\gamma(r_{1th}^2)\gamma(r_{3th}^5)} \quad (15)$$

Compared to (19), we can see that x_1^* is equal to the apex solution of link l_1^2 . It must be emphasized that we identify the optimal value x_1^* at stage 2 of backward DP and that the optimal decision of stage 2 is also the optimal decision when we consider both stage 1 and stage 2 together. This means that our solution complies with the so-called “Principle of Optimality” [39]. Inserting x_1^* to (11), we get the following result.

$$\begin{aligned} x_2^* &= \frac{N\gamma(r_{3th}^5) + G_1^5\gamma(r_{3th}^5)x_1^*}{G_3^5} \\ &= \frac{G_1^2N\gamma(r_{3th}^5) + G_1^5N\gamma(r_{1th}^2)\gamma(r_{3th}^5)}{G_1^2G_3^5 - G_3^2G_1^5\gamma(r_{1th}^2)\gamma(r_{3th}^5)} \end{aligned} \quad (16)$$

Compared to (20), we can see that x_2^* is equal to the apex solution of link l_3^5 . If $0 \leq x_1^*, x_2^* \leq P_{max}$, link l_1^2 and link l_3^5 can transmit simultaneously with rates r_{1th}^2 and r_{3th}^5 , respectively. We observe that the computational complexity of finding the optimal powers is a quadratic function of the number of simultaneous transmissions. Appendix C contains a discussion of extending the proposed dynamic programming method of this section to the case of an arbitrary number of simultaneous transmissions.

In what follows, we elaborate on the details of our power control algorithm. Our algorithm works on specified time slot assignment strategies and is to be executed at the beginning of each time slot. We take DTSA for example here. DTSA is a slot assignment strategy designed for TDMA based ad-hoc networks. It guarantees no pair of nodes within a two-hop neighborhood are assigned to the same slot. We embed two kinds of control packets into DTSA and call them Transmit Requirement Packet (TRP) and Power Information Packet (PIP).

- TRPs are transmitted to the slot owner at the beginning of a slot by the nodes which are not the current slot owner but would like to transmit within that slot. By sending a TRP to the slot owner, a node informs the slot owner about the position of the sender and the receiver. The traffic load and the required r_{th} of the link should be contained in the TRP.
- PIPs are transmitted by the slot owner to inform the calculated powers and rates to the nodes which are permitted to transmit.

At the beginning of the slot, every node within the contention area of the slot owner and interested in transmission sets a random timer. As its timer goes off, the node sends a TRP to inform its intent to transmit to the slot owner. In order to gather this information, the slot owner listens on a control channel for transmission requests from the neighbors for a certain short period of time referred to as τ . The listening period τ is typically set to the first 7% to 10% of the slot duration. In order to statistically guarantee the delivery of transmitted TRPs, the random timer r_i at node i is set as follows.

$$r_i = t_0 + 0.07T + r \quad 0 \leq r \leq 0.03T \quad (17)$$

where t_0 represents the beginning of a time slot, T is the length of the time slot, and r is a number selected randomly. Per Equation (17), the slot owner processes transmission requests that arrive between 2.1 ms and 3 ms after the start of its time slot on a first-come first-serve basis. Late requests will not be processed. Upon the receipt of a TRP accepted for processing, the slot owner begins to evaluate whether a node can be granted permission to simultaneously transmit in its slot. If two simultaneous transmissions can be established, the slot owner evaluates whether a third transmission can be permitted upon the receipt of a second request. If the first request could not be granted, the slot owner still evaluates the possibility of granting permission to transmit in response to the second request independent of the first request. The process continues this way, i.e., upon the receipt of a new request within the period of τ . The slot owner assigns data rates as follows attempting to address the trade off between power efficiency and throughput. First, it assigns itself the highest data rate possible, not to exceed r_{max} , the rate that can finish its transmission within that slot. For other links, the slot owner just assigns rates equal to the required r_{th} of those links. If the slot owner has no packet to transmit, the first request will receive the highest priority, but the slot owner is still responsible for evaluating the requests and granting permissions to transmit. The slot owner will stop evaluating transmission requests, hand out the results of evaluations through broadcast PIPs to its neighbors, and begin transmitting. The other nodes granted permission to transmit will begin transmitting after receiving notification from the slot owner using the optimal transmission powers and the data rates as dictated by the slot owner. Our optimal power control algorithm at a given slot is described below.

From the description of the algorithm, it is observed that the computational complexity is specified by step 3. If there are a total of L active links in the network, the computational complexity of the algorithm is in the order of $\mathcal{O}((L/s)^2)$ where s is the same as defined in [31]. The complexity is lower than that of DPRL which is in the order of $\mathcal{O}(m + (L/s)^2)$. This low computational complexity is important for us to realize objective (i) and objective (iii) mentioned in section III. In the next section, our simulation results show that the number of simultaneous transmissions is most closely tied to the relative position of the transmitting nodes and corresponding receivers.

Algorithm 1 : Optimal Power Control Algorithm

- 1: The time slot assignment policy and clock synchronization are initialized at the startup of the protocol.
 - 2: At the beginning of one slot, the slot owner collects the TRPs from other nodes in its contention area.
 - 3: The slot owner assigns every requirement a priority and calculates the optimal powers using dynamic programming method according to the priority of the request.
 - 4: The slot owner hands out the PIPs at the end of period of τ or after processing all collected TRPs and begins transmitting with data rate r_{max} .
 - 5: The other nodes granted permission in the contention area begin to transmit with a data rate r_{th} .
-

V. EXPERIMENTS ANALYSIS

To study the performance effects of our OPC algorithm on STDMA MAC protocols, we carry out numerical experiments in NS3. We use DTSA and USAP-MA as non-STDMA benchmarks and DPRL as an STDMA benchmark for evaluating the performance of our algorithm. By setting frame length as a power 2 of slots, DTSA and USAP provide collision-free packet transmission among nodes with different frame lengths. We embed our OPC algorithm into DTSA and USAP-MA and refer to them as OPC-DTSA and OPC-USAP, respectively. We note that our power control algorithm does not change the frame format of any underlying TDMA protocol. The slot length is set to 30 ms, the operation duration of the OPC algorithm is limited to 3 ms, and we experiment with fixed length data packets of size 512 bytes. Each sender can choose one of five transmission rates in the set $\{r_1 = 1, r_2 = 3, r_3 = 5, r_4 = 7, r_5 = 9\}$ packets/slot. For experimental convenience, one slot duration is assumed to be equal to the transmission time of one packet at the lowest rate. We examine five different scenarios by selecting distinct path loss exponents, i.e., θ in Equation (2). The latter means that the network operates in 5 different environments from line of sight free space to indoor environment. The path loss exponent influences the maximum transmission range under different rates, the slot assignment strategy of all protocols, and the performance of our algorithm. In essence, a higher value of θ means a higher spatial reuse factor. The value of P_{max} is set to 30 dBm and the average thermal noise N is -50 dBm. We use Shannon's channel capacity formula to calculate the corresponding $SINR$ threshold at different rates. The farthest transmission ranges corresponding to rates for different values of θ are shown in Table I. The values of r_{max} and r_{th} are assigned based on the parameter settings of the table. In each time of our experiments, we generate the network topology by distributing 100 stationary nodes independently and uniformly in a square area of dimensions 400×400 square meters. Our simulation program randomly selects 30 links formed by these nodes on which communications can be established at the lowest rate under all the path loss exponents.

To test the performance of OPC under high traffic loads, we first compare the performance of the five algorithms DTSA, USAP-MA (referred to as USAP for brevity), OPC-DTSA,

TABLE I
TRANSMISSION RANGES CALCULATED BY SHANNON'S CHANNEL CAPACITY FORMULA.

C	$SINR_{threshold}$	$d_{max}(\theta = 2)$	$d_{max}(\theta = 2.5)$	$d_{max}(\theta = 3)$	$d_{max}(\theta = 3.5)$	$d_{max}(\theta = 4)$
1	1	10000	1584	464	193	100
3	7	3779	727	243	111	61
5	31	1796	401	147	72	42
7	127	887	228	92	48	30
9	511	442	131	58	32	21

OPC-USAP, and DPRL in a saturated network operating scenario in which all nodes have traffic to transmit at any time. In OPC-USAP and OPC-DTSA, each link uses the highest data rate that it can use as its r_{th} if permitted to simultaneously transmit with a slot owner. The reported results are the steady-state averages associated with 50 simulation runs of thirty minutes or longer. Considering different values of path loss exponent θ , Fig. 4 illustrates the network throughput of these five algorithms as a function of θ . It can be observed that USAP has the lowest throughput performance as its slot assignment strategy allows for having a large number of unassigned slots. The same argument also justifies the fact that the throughput performance of OPC-USAP is lower than that of OPC-DTSA and DPRL. For $\theta = 2$, there is almost no performance difference between USAP and OPC-USAP. At that point, the performance of DTSA, DPRL, and OPC-DTSA are almost the same. That is because high interference renders simultaneous transmissions nearly impossible for small values of θ . However, when θ is greater than 2.5, the throughput under OPC-USAP and OPC-DTSA are on average more than 2 times better than those attained by the associated original algorithms. At the same time, OPC-DTSA is outperforming DPRL since optimal power values decrease interference thereby allowing for more simultaneous transmissions compared to DPRL. Noticeable performance improvements are realized under OPC-USAP, OPC-DTSA, and DPRL as θ increases to 3.5 and 4 since more links can transmit within same slots. Practically, OPC-USAP, OPC-DTSA, and DPRL can offer simultaneous transmissions in up to 4 contention areas when the path loss exponents are 3.5 and 4. Fig. 5 shows the average PER corresponding to Fig. 4. Although the values of PER fluctuate due to the variations of the radio channels and random formation of the links, the general trend is increasing. The main reason is that increasing spatial reuse results in increasing interference from nodes both inside and outside of the LCA. Due to interference caused by simultaneous transmissions, the PER of OPC-USAP and OPC-DTSA are both higher than their associated original protocols. Since DPRL utilizes high transmission powers, it outperforms both OPC-USAP and OPC-DTSA. Even though, the packet loss rate of OPC-USAP and OPC-DTSA are both relatively low and do not lower the throughput significantly.

Fig. 6 depicts the average power consumption for transmitting one packet under 5 different values of θ when the network is saturated. The curves labeled OPC-USAP-LB and OPC-DTSA-LB are both drawn under the assumption that USAP and DTSA communication links use the lowest power levels satisfying the corresponding SINR threshold constraints. Under such assumption, the power consumption results are the

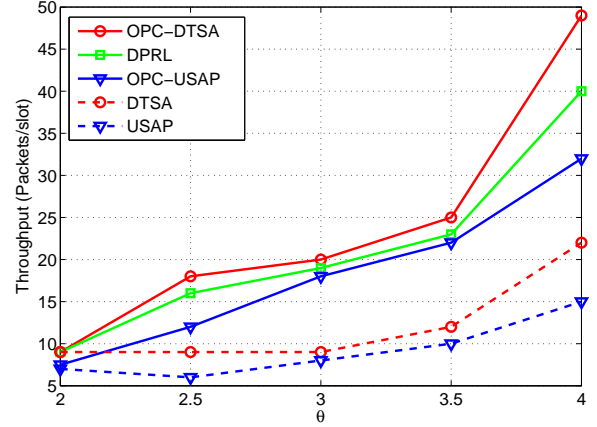


Fig. 4. The throughput comparison of USAP, DTSA, OPC-USAP, OPC-DTSA, and DPRL for 5 different path loss scenarios when the network is saturated.

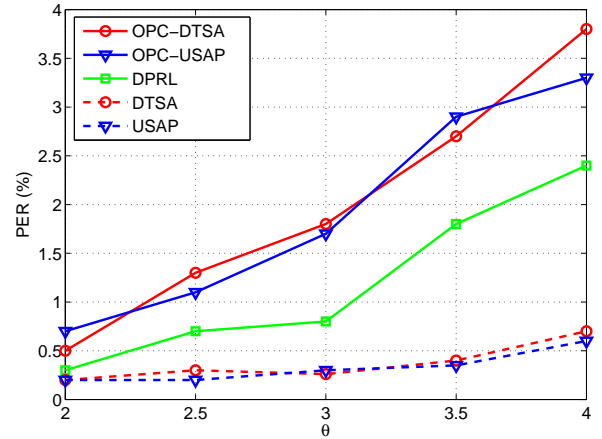


Fig. 5. The PER comparison of USAP, DTSA, OPC-USAP, OPC-DTSA, and DPRL for 5 different path loss scenarios when the network is saturated.

lower bounds of OPC-USAP and OPC-DTSA. As expected, the power consumption increases when increasing the path loss exponent. The power consumption of OPC-USAP and OPC-DTSA are a little higher than the associated original algorithms in all scenarios. That is because although with our OPC algorithm OPC-USAP and OPC-DTSA minimize the interference between simultaneous transmissions, they do not completely eliminate interference. At the same time, the power consumption of DPRL is much higher than that of OPC-USAP and OPC-DTSA. This is due to the fact that DPRL uses very high powers in order to achieve high data rates thereby

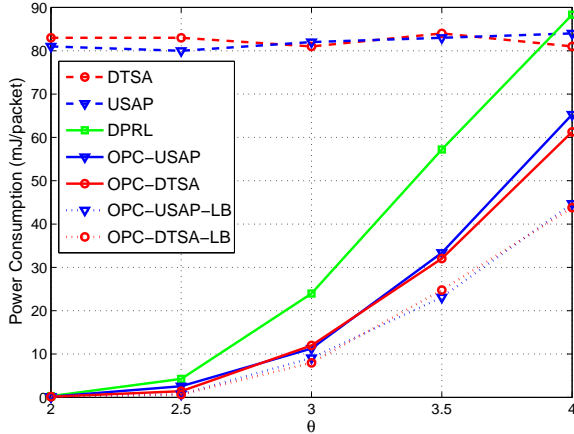


Fig. 6. The power consumption comparison of USAP, DTSA, OPC-USAP, OPC-DTSA, and DPRL for 5 different path loss scenarios when the network is saturated. The curve labels ending at LB specify the power lower bounds of optimal single transmission.

significantly increasing mutual interference.

While not shown here, similar pattern of results are observed when experimenting with data packets of fixed sizes 64, 128, and 256. We have observed that the throughput of all algorithms are decreased while the associated power consumptions and *PER* measures are increased as the packet length is reduced. The differences are of higher significance in environments for which the value of θ exceeds 3. Further and with the reduction of packet size, throughput, power, and *PER* measures of OPC-USAP and OPC-DTSA are more significantly affected than the other algorithms due to a higher overhead of control packets exchanged.

To evaluate the performance of OPC under light traffic loads, we run another set of simulations in which we compare the performance of the same five algorithms. In each experiment, we assume that each sender of the randomly selected 30 links has 100 packets to transmit. We record the completion time and calculate the corresponding throughput, *PER* and power consumption for transmitting all packets. In OPC-USAP and OPC-DTSA, each sender selects the data rate r_{th} that can finish its traffic load in a slot. If that is not possible, the highest available data rate is chosen as r_{th} . The slot owners' data rate r_{max} is assigned according to the same principle. As before, each data point is averaged over 50 simulation runs. The results for the average transfer times are shown in Fig. 7. Similar to the saturated case, the OPC-DTSA has the best performance followed by DPRL and OPC-USAP. We note that completion times are expected to fluctuate from case to case depending on random placement of the links. Regardless, OPC offers significant performance improvements to both USAP and DTSA.

The throughput attained by the five algorithms is shown in Fig. 8. The most significant observation is that the throughput performance gaps between OPC-USAP, OPC-DTSA and the associated original algorithms are much higher than those in saturated networks. That is because when the network is not saturated, USAP-MA and DTSA can waste many idle

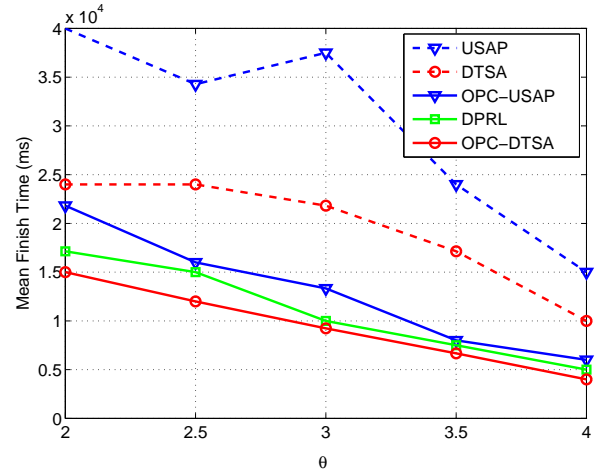


Fig. 7. The mean transfer time comparison of USAP, DTSA, OPC-USAP, OPC-DTSA, and DPRL for 5 different path loss scenarios when the traffic load is light.

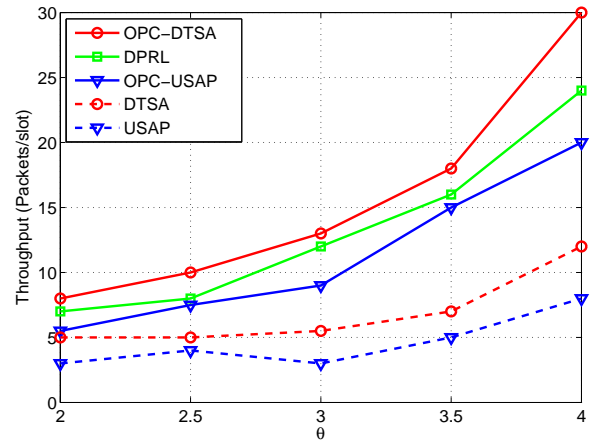


Fig. 8. The throughput comparison of USAP, DTSA, OPC-USAP, OPC-DTSA, and DPRL for 5 different path loss scenarios when the traffic load is light.

slots. To the contrary, not only OPC-USAP and OPC-DTSA use the idle slots but also establish multiple simultaneous transmissions in those slots. Fig. 9 is the average *PER* performance corresponding to Fig. 8. As observed, the curves exhibit the same general trend as those of saturated networks. The most notable observation is that the gaps between OPC-USAP, OPC-DTSA, and the other three algorithms are much lower than those in saturated networks. This is due to mutual interference decrease associated with decreasing simultaneous transmissions in the same slot. Accordingly, we argue that our power control algorithm is able to perform well under different traffic loads and types. At the same time, considering the parameter settings in our experiments, we can also argue that applying our power control algorithm into the existing STDMA MAC protocols is practical.

The power consumptions of the five algorithms under light traffic load are compared in Fig. 10. We can see that the gaps between the power consumption of the two OPC algorithms

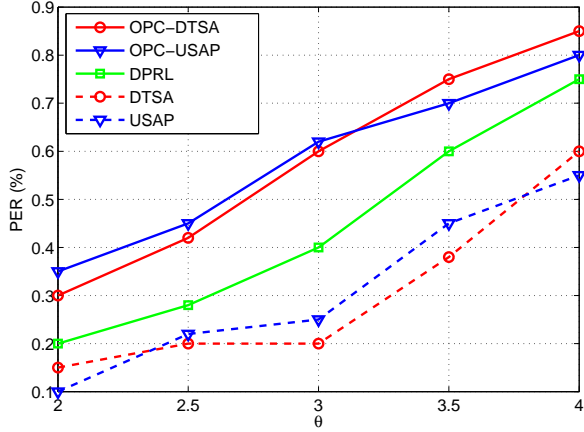


Fig. 9. The PER comparison of USAP, DTSA, OPC-USAP, OPC-DTSA, and DPRL for 5 different path loss scenarios when the traffic load is light.

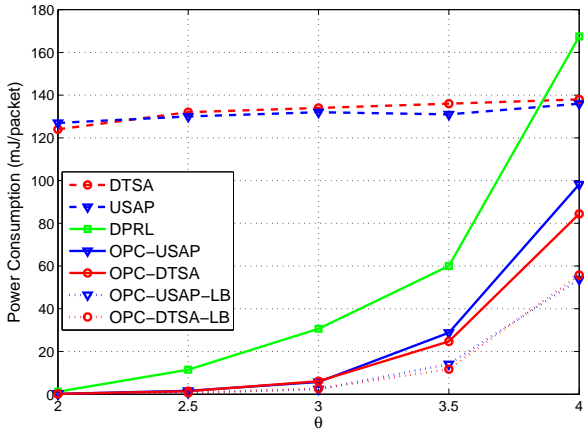


Fig. 10. The power consumption comparison of USAP, DTSA, OPC-USAP, OPC-DTSA, and DPRL for 5 different path loss scenarios when the traffic load is light. The curve labels ending at LB specify the power lower bounds of optimal single transmission.

and DPRL are higher compared to the saturation experiments. This is because at low transmit rates, OPC-USAP and OPC-DTSA assign each link the corresponding optimal power which results in higher energy efficiency but DPRL still uses high powers and hence offers a low energy efficiency.

As the subject of our ongoing future work, we end this section by providing a brief discussion of the effects of mobility on the operation of OPC. To that end, we note that mobility introduces changes in two-hop neighborhoods requiring updates to the two-hop neighborhood information stored in each node. The latter can potentially result in changing the slot assignment of the underlying MAC protocol thereby influencing OPC strategy accordingly. In addition, mobility leads to frequent rate changes thereby invalidating the calculated optimal powers associated with simultaneous transmissions. The latter requires re-calculation of the OPC results and significant packet delivery delay. Lastly, mobility can lead to a deterioration of link quality making data transmission prone to failure. This can worsen the effectivity of

OPC as the result of delivery failure associated with lowered SINR values and increasing the rate of packet retransmission.

VI. CONCLUSION

In this paper, we proposed a highly energy efficient power control algorithm under rate and SINR constraints. Our algorithm maximized the number of simultaneous transmissions for a variety of STDMA time slot assignment strategies used in multi-hop wireless networks. We developed a new mathematical programming formulation for the problem first and then proved an approximated mathematical relationship between data rates and power levels used by successful simultaneous transmissions. Based on our proof, we derived an equivalent linear programming formulation to the problem and solved it using dynamic programming. We then proposed a practical low complexity power control algorithm based on the optimal solution. We showed that our proposed power control algorithm can generate a simultaneous transmission schedule for slot owners and specify the corresponding minimal powers with a low computational complexity. We then applied our power control algorithm to USAP and DTSA protocols and compared the performance of the resulting STDMA protocols to those of their original counterparts as well as DPRL algorithm. We showed that our power control algorithm can significantly improve power consumption, throughput, and delay (completion time) performance of STDMA networks under different network traffic loads.

Currently, we are in process of extending our work to cover propagation models accounting for time-varying fading channels, offering priority mechanisms beyond the first come first serve choices of accommodating transmitting nodes, and finally capturing the effects of mobility.

APPENDIX A PROOF OF THEOREM 1

Proof: We open this appendix by noting that the proof provided below is generically applicable to any pair of arbitrary pair of links. According to the topology of Fig. 1, the following constraints need to be satisfied in order to make two simultaneous transmissions l_1^2 and l_3^5 successful.

$$\begin{cases} G_1^2 P_1^2 - \gamma(r_1^2) G_3^2 P_3^5 \geq \gamma(r_1^2) N_2 \\ G_3^5 P_3^5 - \gamma(r_3^5) G_1^2 P_1^2 \geq \gamma(r_3^5) N_5 \end{cases} \quad (18)$$

Apex solution: According to [28] and [29], the apex solution of the linear inequalities (18) are the power values \bar{P}_1^2, \bar{P}_3^5 that satisfy linear inequalities in equality forms. Based on the ‘‘Perron-Frobenius’’ theorem, [28] and [29] proved that the following statements are equivalent:

(a) linear inequalities (18) have a nonnegative solution, i.e., P_1^2, P_3^5 are both nonnegative.

(b) The apex solution of linear inequalities (18) is nonnegative, i.e., \bar{P}_1^2, \bar{P}_3^5 are both nonnegative.

At the same time, according to ‘‘Perron-Frobenius’’ theorem, if statement (a) or (b) is valid, then $P_1^2 \geq \bar{P}_1^2, P_3^5 \geq \bar{P}_3^5$, where \bar{P}_1^2, \bar{P}_3^5 is an arbitrary nonnegative solution of linear inequalities (18). Based on the statements above, two links can transmit in the same time slot if and only if:

$$0 \leq (\bar{P}_1^2 = \frac{G_3^5 N_2 \gamma(r_1^2) + G_3^2 N_5 \gamma(r_1^2) \gamma(r_3^5)}{G_1^2 G_3^5 - G_3^2 G_1^5 \gamma(r_1^2) \gamma(r_3^5)}) \leq P_{max} \quad (19)$$

and

$$0 \leq (\bar{P}_3^5 = \frac{G_1^2 N_5 \gamma(r_3^5) + G_1^5 N_2 \gamma(r_1^2) \gamma(r_3^5)}{G_1^2 G_3^5 - G_3^2 G_1^5 \gamma(r_1^2) \gamma(r_3^5)}) \leq P_{max} \quad (20)$$

Hence, we know that the apex solution is the smallest power pair offering stable transmissions to both senders. The existence of the apex solution is equivalent to the existence of other solutions. Hence, if the apex solution is a non-negative monotonically increasing convex function of its own rate and the other sender's rate, then any other solution which can offer a stable simultaneous transmission schedule for both senders is at least a non-negative monotonically increasing convex function of the two rates. In other words, any other solution which can offer a successful simultaneous transmission schedule to l_1^2 and l_3^5 at the required data rates has the same relationship with the data rates as the apex solution does. Compliance with relationship (19) and (20) is then equivalent to compliance with the following relationships.

$$G_1^2 G_3^5 - G_3^2 G_1^5 \gamma(r_1^2) \gamma(r_3^5) > 0 \quad (21)$$

and

$$\bar{P}_1^2 = \frac{G_3^5 N_2 \gamma(r_1^2) + G_3^2 N_5 \gamma(r_1^2) \gamma(r_3^5)}{G_1^2 G_3^5 - G_3^2 G_1^5 \gamma(r_1^2) \gamma(r_3^5)} \leq P_{max} \quad (22)$$

From "Taylor's Theorem" [44], we can assume that the relationship between $\gamma(r)$ and r can be expressed by as follows.

$$\gamma(r) = \lambda_n r^n + \lambda_{n-1} r^{n-1} + \dots + \lambda_2 r^2 + \lambda_1 r + \lambda_0 \quad (23)$$

In the equation above, $\lambda_n, \lambda_{n-1}, \dots, \lambda_0 \geq 0$. Under the best condition of the channel, we can assume a linear function $\gamma(r) = \lambda_1 r + \lambda_0$ implying that Equation (23) has at least a first-order derivative ($\lambda_1 > 0$). Thus, for the apex solution below

$$\bar{P}_1^2 = \frac{G_3^5 N_2 \gamma(r_1^2) + G_3^2 N_5 \gamma(r_1^2) \gamma(r_3^5)}{G_1^2 G_3^5 - G_3^2 G_1^5 \gamma(r_1^2) \gamma(r_3^5)} \quad (24)$$

the first-order derivative with respect to r_3^5 exists. Defining $x = \gamma(r_1^2) > 0$, $y = \gamma(r_3^5) > 0$, $r_3^5 = t$, and $\bar{P}_1^2 = f(x, y(t))$, we get

$$\begin{aligned} \frac{\partial \bar{P}_1^2}{\partial r_3^5} &= \frac{\partial f}{\partial y} \cdot \frac{dy}{dt} \\ &= \frac{G_3^2 N_5 x y' (G_1^2 G_3^5 - G_3^2 G_1^5 x y)}{(G_1^2 G_3^5 - G_3^2 G_1^5 x y)^2} \\ &\quad + \frac{G_3^2 G_1^5 x y' (G_3^5 N_2 x + G_3^2 N_5 x y)}{(G_1^2 G_3^5 - G_3^2 G_1^5 x y)^2} \end{aligned} \quad (25)$$

From (21), we know that the denominator of (25) is greater than zero. On the other hand, regardless of the type of channel state, y' exists with $y' > 0$, $x > 0$, $y > 0$. Therefore, $\frac{\partial \bar{P}_1^2}{\partial r_3^5}$ exists and $\frac{\partial \bar{P}_1^2}{\partial r_3^5} > 0$. This mean the apex solution \bar{P}_1^2 is a monotonically increasing function of t .

Assume that t_1 and t_2 are arbitrary in $(0, \infty)$ and $t_2 > t_1$, denote $\frac{t_2 + t_1}{2} = t_0$ and $t_2 - t_0 = t_0 - t_1 = h$, then $t_1 = t_0 - h$,

$t_2 = t_0 + h$. From the proofs above, we know $\frac{\partial f}{\partial t}$ exists. Then, we get the following two equations according to "Lagrange Mean Value Theorem" [44].

$$f(x, y(t_0 + h)) - f(x, y(t_0)) = \frac{\partial f}{\partial y} \cdot \frac{dy}{dt}(x, y(t_0 + \theta_1 h)) \cdot h \quad (26)$$

$$f(x, y(t_0)) - f(x, y(t_0 - h)) = \frac{\partial f}{\partial y} \cdot \frac{dy}{dt}(x, y(t_0 - \theta_2 h)) \cdot h \quad (27)$$

In the equations above, $0 < \theta_1 < 1$, $0 < \theta_2 < 1$. Subtracting (27) from (26), we get:

$$\begin{aligned} &f(x, y(t_0 + h)) + f(x, y(t_0 - h)) - 2f(x, y(t_0)) \quad (28) \\ &= \left(\frac{\partial f}{\partial y} \cdot \frac{dy}{dt}(x, y(t_0 + \theta_1 h)) - \frac{\partial f}{\partial y} \cdot \frac{dy}{dt}(x, y(t_0 - \theta_2 h)) \right) \cdot h \end{aligned}$$

Following the same procedure as that in the proof of (25), it is easy to see that $\frac{\partial f}{\partial y} \cdot \frac{dy}{dt}$ is still a monotonically increasing function of t . Accordingly,

$$\frac{\partial f}{\partial y} \cdot \frac{dy}{dt}(x, y(t_0 + \theta_1 h)) - \frac{\partial f}{\partial y} \cdot \frac{dy}{dt}(x, y(t_0 - \theta_2 h)) > 0 \quad (29)$$

Then,

$$\frac{f(x, y(t_0 + h)) + f(x, y(t_0 - h))}{2} > f(x, y(t_0)) \quad (30)$$

implying

$$\frac{f(x, y(t_1)) + f(x, y(t_2))}{2} > f(x, y(\frac{t_1 + t_2}{2})) \quad (31)$$

Thus, f is a strictly monotonically increasing convex function of t . Using the same principle, we can prove that \bar{P}_1^2 is a strictly monotonically increasing convex function of r_1^2 and \bar{P}_3^5 is a strictly monotonically increasing convex function of r_1^2 and r_3^5 . This relationship is shown in Fig.3. ■

APPENDIX B PROOF OF THEOREM 2

Just like the previous appendix, we open by noting that the proof provided below is generically applicable to any pair of arbitrary pair of links.

Proof: Assume that l_1^2 and l_3^5 are two arbitrary links that are contained in this L simultaneous transmissions. Based on (1), we can rewrite the required SINR threshold at the receiver nodes 2 and node 5 as follows.

$$\frac{P_1^2 G_1^2}{P_3^5 G_3^2 + (\sum I_k^j + N_2)} \geq \gamma(r_1^2), \quad j \neq k \neq 3 \quad (32)$$

$$\frac{P_3^5 G_3^5}{P_1^2 G_1^5 + (\sum I_p^q + N_5)} \geq \gamma(r_3^5), \quad j \neq k \neq p \neq q \neq 1 \quad (33)$$

Then, based on (32) and (33), we can get the apex solution of P_1^2 and P_3^5 under this L simultaneous transmissions as follows.

$$\bar{P}_{1L}^2 = \frac{G_3^5 (\sum I_k^j + N_2) \gamma(r_1^2) + G_3^2 (\sum I_p^q + N_5) \gamma(r_1^2) \gamma(r_3^5)}{G_1^2 G_3^5 - G_3^2 G_1^5 \gamma(r_1^2) \gamma(r_3^5)} \quad (34)$$

and

$$\bar{P}_{3L}^5 = \frac{G_1^2 (\sum I_p^q + N_5) \gamma(r_3^5) + G_1^5 (\sum I_k^j + N_2) \gamma(r_1^2) \gamma(r_3^5)}{G_1^2 G_3^5 - G_3^2 G_1^5 \gamma(r_1^2) \gamma(r_3^5)} \quad (35)$$

Comparing (34) and (35) to (19) and (20), it is easy to see that the differences between the apex solutions of P_1^2 and P_3^5 under two simultaneous transmissions and L simultaneous transmissions are $(\sum I_k^j + N_2)$ and $(\sum I_p^q + N_5)$, respectively. From the proof of Theorem 1, we know that we can deal with the terms $(\sum I_k^j + N_2)$ and $(\sum I_p^q + N_5)$ just like the terms N_2 and N_5 implying that they do not influence the results of the proof. This means that in the case of L simultaneous transmissions, the relationship between P_1^2 and r_1^2, r_3^5 as well as the relationship between P_3^5 and r_1^2, r_3^5 are the same as that of a case in which l_1^2 and l_3^5 are the only pair of simultaneous transmissions. Based on Theorem 1 and considering l_1^2 and l_3^5 are two arbitrary links in the case of L simultaneous transmissions, we conclude that the power used by one link is a non-negative monotonically increasing convex function of its own rate and any one of other rates in the case of L simultaneous transmissions. Then, applying ‘‘Jensen’s inequality’’ [45] to the case of L simultaneous transmissions, we conclude that the highest power efficiency is obtained at the DRTP. ■

APPENDIX C

HOW TO SPECIFY THE OPTIMAL POWERS FOR AN ARBITRARY NUMBER OF SIMULTANEOUS TRANSMISSIONS

The problem in hand is identified as shown below.

$$\begin{cases} f_k(S_k) = \min_{x_k \in S_k} \{x_k + f_{k+1}(S_{k+1})\} \\ f_{n+1}(S_{n+1}) = 0 \end{cases} \quad (36)$$

When $k = n$,

$$\begin{aligned} f_n(S_n) &= \min_{x_n \in S_n} \{x_n + f_{n+1}(S_{n+1})\} \\ &= \min_{x_n \in S_n} \{x_n\} \\ &= \min\left\{\frac{R_{n,n}}{a_{n,n}}, \min\left(\frac{-R_{1,n}}{|a_{1,n}|}, \frac{-R_{2,n}}{|a_{2,n}|}, \dots, \frac{-R_{n-1,n}}{|a_{n-1,n}|}\right)\right\} \end{aligned} \quad (37)$$

where the last step follows from

$$\frac{R_{n,n}}{a_{n,n}} \leq x_n \leq \min\left\{\frac{-R_{1,n}}{|a_{1,n}|}, \frac{-R_{2,n}}{|a_{2,n}|}, \dots, \frac{-R_{n-1,n}}{|a_{n-1,n}|}\right\} \quad (38)$$

We get x_n^* when,

$$\frac{R_{n,n}}{a_{n,n}} = \min\left\{\frac{-R_{1,n}}{|a_{1,n}|}, \frac{-R_{2,n}}{|a_{2,n}|}, \dots, \frac{-R_{n-1,n}}{|a_{n-1,n}|}\right\} \quad (39)$$

where x_n^* can be shown as

$$x_n^* = f(R_{i,n}, a_{i,n}), \quad i \in \{1, \dots, n\} \quad (40)$$

When $k = n - 1$,

$$f_{n-1}(S_{n-1}) = \min_{x_{n-1} \in S_{n-1}} \{x_{n-1} + f_n(S_n)\} \quad (41)$$

Since

$$R_{in} = R_{i,n-1} - a_{i,n-1}x_{n-1}, \quad i \in \{1, \dots, n\} \quad (42)$$

We conclude that x_{n-1}^* is derived when it satisfies Equation (39). By inserting (42) into (39), we get,

$$\begin{aligned} \frac{R_{n,n-1} - a_{n,n-1}x_{n-1}^*}{a_{n,n}} &= \min\left\{\frac{R_{1,n-1} - a_{1,n-1}x_{n-1}^*}{|a_{1,n}|}, \right. \\ &\left. \frac{R_{2,n-1} - a_{2,n-1}x_{n-1}^*}{|a_{2,n}|}, \dots, \frac{R_{n-1,n-1} - a_{n-1,n-1}x_{n-1}^*}{|a_{n-1,n}|}\right\} \end{aligned} \quad (43)$$

At the same time, x_{n-1}^* has to comply with its own state shown below.

$$\begin{aligned} \frac{R_{n-1,n-1}}{a_{n-1,n-1}} &\leq x_{n-1}^* \\ &\leq \min\left\{\frac{-R_{1,n-1}}{|a_{1,n-1}|}, \frac{-R_{2,n-1}}{|a_{2,n-1}|}, \dots, \frac{-R_{n-2,n-1}}{|a_{n-2,n-1}|}\right\} \end{aligned} \quad (44)$$

Then, x_{n-1}^* can be shown as follows.

$$x_{n-1}^* = f(R_{i,n-1}, a_{i,n-1}, a_{i,n}), \quad i \in \{1, \dots, n\} \quad (45)$$

Applying the same recursion as shown above, we can get the optimal power at stage k ($1 < k < n$).

$$x_k^* = f(R_{i,k}, a_{i,k}, a_{i,k+1}, \dots, a_{i,n-1}, a_{i,n}), \quad i \in \{1, \dots, n\} \quad (46)$$

When the recursion reaches the first stage, we can obtain x_1^* as below.

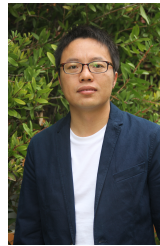
$$x_1^* = f(R_{i,1}, a_{i,1}, a_{i,2}, \dots, a_{i,n-1}, a_{i,n}), \quad i \in \{1, \dots, n\} \quad (47)$$

Since all $R_{i,1}$ and $a_{i,k}$ values with $(i, k = 1, 2, \dots, n)$ are given constant numbers, we can obtain x_1^* from (47). Then, we insert x_1^* to the equation of x_2^* in order to get x_2^* , we insert x_2^* to the equation of x_3^* in order to get x_3^* , and so on. We continue this process until reaching to (40) and identifying all optimal powers for n simultaneous transmissions.

REFERENCES

- [1] S. Ahmed and A. Ramani, ‘‘Exploring the requirements for QoS in mobile ad hoc networks,’’ *J. Inf. Commun. Technol.*, vol. 1, no. 2, pp. 1-9, 2007.
- [2] T. -S. Kim, Y. Yang, J. C. Hou, ‘‘Resource allocation for QoS support in wireless mesh networks,’’ *IEEE Trans. Wireless Commun.*, vol. 12, no. 5, pp. 2046-2054, May 2013.
- [3] M. Zafer, ‘‘Dynamic rate-control and scheduling algorithms for quality-of-service in wireless networks,’’ Ph.D. dissertation, Dept. Elect. Eng. Comput. Sci., Massachusetts Inst. Technol. (MIT), Cambridge, MA, 2007.
- [4] M. Masihpour and J. Agbinya, ‘‘Planning of WiMAX and LTE networks,’’ University of Technology, Sydney Australia, 2011.
- [5] N. Salodkar, A. Karandikar, V. S. Borkar, ‘‘A stable online algorithm for energy-efficient multiuser scheduling,’’ *IEEE Trans. Mobile Comput.*, vol. 9, no. 10, pp. 1391-1406, Oct. 2010.
- [6] Y. Huang, C. W. Tan, and B. D. Rao, ‘‘Joint beamforming and power control in coordinated multicell: max-min duality, effective network and large system transition,’’ *IEEE Trans. Wireless Commun.*, vol. 12, no. 6, pp. 2730-2742, Jun. 2013.
- [7] M. Barceló, A. Correa, J. L. Vicario and A. Morell, ‘‘Joint routing, channel allocation and power control for real-life wireless sensor networks,’’ to be published on *Trans. Emerging Tel. Tech.* (2014), doi: 10.1002/ett.2783.
- [8] M. Wiczanowski, H. Boche, and S. Stanczak, ‘‘An algorithm for optimal resource allocation in cellular networks with elastic traffic,’’ *IEEE Trans. Commun.*, vol. 57, no. 1, pp. 41-44, Jan. 2009.
- [9] P. Gupta and P. R. Kumar, ‘‘The capacity of wireless networks,’’ *IEEE Trans. Inf. Theory*, vol. 46, no. 2, pp. 388-404, Mar. 2000.
- [10] A. Muqattash and M. Krunz, ‘‘A single-channel solution for transmission power control in wireless ad hoc networks,’’ in *Proc. ACM Int. Symp. Mobile Ad Hoc Networking Computing*, 2004, pp. 210-221.
- [11] P. Li, X. Geng, and Y. Fang, ‘‘An adaptive power controlled MAC protocol for wireless ad hoc networks,’’ *IEEE Trans. Wireless Commun.*, vol. 8, no. 1, pp. 226-233, Jan. 2009.
- [12] F. Rashid-Farrokh and K. J. R. Liu, and L. Tassiulas, ‘‘Downlink power control and base station assignment’’, *IEEE Commun. Lett.*, vol. 1, no. 4, pp. 102-104, Jul. 1997.
- [13] S. Ulukus and R. Yates, ‘‘Stochastic power control for cellular radio systems’’, *IEEE Trans. Commun.*, vol. 46, no. 6, pp. 784-798, Jun. 1998.

- [14] S. -J. Oh and K.M. Wasserman, "Optimality of greedy power control and variable spreading gain in multi-class CDMA mobile networks," in *Proc. ACM/IEEE Mobicom'99*, pp. 102-112, 1999.
- [15] J. Zander, "Distributed cochannel interference control in cellular radio systems," *IEEE Trans. Veh. Technol.*, vol. 41, no. 3, pp. 305-311, Aug. 1992.
- [16] G. J. Foschini and Z. Miljanic, "A simple distributed autonomous power control algorithm and its convergence," *IEEE Trans. Veh. Technol.*, vol. 42, no. 4, pp. 641-646, Nov. 1993.
- [17] R. D. Yates, "A framework for uplink power control in cellular radio systems," *IEEE J. Select. Areas Commun.*, vol. 13, no. 7, pp. 1341-1348, Sept. 1995.
- [18] C. U. Saraydar, N. B. Mandayam, and D. J. Goodman, "Pricing and power control in a multi-cell wireless data network," *IEEE J. Select. Areas Commun.*, vol. 19, no. 10, pp. 1883-1892, Oct. 2001.
- [19] M. Xiao, N. B. Shroff, and E. K. P. Chong, "Utility-based power control in cellular wireless systems," in *Proc. IEEE INFOCOM*, 2001, pp. 412-421.
- [20] J. P. Monks, V. Bhargavan, and W. W. Hwu, "A power controlled multiple access protocol for wireless packet networks," in *Proc. IEEE INFOCOM*, 2001, pp. 219-228.
- [21] H. -C. Luo, E. H. -K. Wu and G.-H. Chen, "A transmission power/rate control scheme in CSMA/CA-based wireless ad hoc networks," *IEEE Trans. Veh. Technol.*, vol. 62, no. 1, pp. 427-431, Jan. 2013.
- [22] E. -S. Jung and N. H. Vaidya, "A power control MAC protocol for ad hoc networks," in *Proc. ACM MOBICOM*, 2002, pp. 36-47.
- [23] A. Maqattash and M. Krunz, "Power controlled dual channel (PCDC) medium access protocol for wireless ad hoc networks," in *Proc. IEEE INFOCOM*, 2003, pp. 470-480.
- [24] R. L. Cruz and A. V. Santhanam, "Optimal routing, link scheduling and power control in multi-hop wireless networks," in *Proc. IEEE INFOCOM*, 2003, pp. 702-711.
- [25] T. Elbatt and A. Ephremides, "Joint Scheduling and Power Control for Wireless Ad Hoc Networks," *IEEE Trans. Wireless Commun.*, vol. 3, no. 1, pp. 74-85, Jan. 2004.
- [26] A. Behzad and I. Rubin, "Impact of power control on the performance of ad hoc wireless networks," in *Proc. IEEE INFOCOM*, 2005, pp. 102-113.
- [27] J. Kim, S. Kim, S. Choi, and D. Qiao, "CARA: Collision-aware rate adaptation for IEEE 802.11 WLANs," in *Proc. IEEE INFOCOM*, 2006, pp. 1-11.
- [28] A. Behzad and I. Rubin, "Optimum integrated link scheduling and power control for multi-hop wireless networks," *IEEE Trans. Veh. Technol.*, vol. 56, no. 1, pp. 194-205, Jan. 2007.
- [29] K. Hedayati, A. Behzad, and I. Rubin, "Integrated power controlled rate adaptation and medium access control in wireless mesh networks," *IEEE Trans. Wireless Commun.*, vol. 9, no. 7, pp. 2362-2370, Jul. 2010.
- [30] K. Hedayati and I. Rubin, "Integrated power controlled adaptive rate link scheduling in wireless mesh networks," in *Proc. IEEE Globecom*, 2010, pp. 1-5.
- [31] K. Hedayati and I. Rubin, "A robust distributive approach to adaptive power and adaptive rate link scheduling in wireless mesh networks," *IEEE Trans. Wireless Commun.*, vol. 11, no. 1, pp. 275-283, Jan. 2012.
- [32] A. Kanzaki, T. Uemukai, T. Hara, and S. Nishio, "Dynamic TDMA slot assignment in ad hoc networks," in *Proc. 17th Int. Conf. Advanced Inf. Networking, Applicat.*, 2003, pp. 330-335.
- [33] C. D. Young, "USAP multiple access: dynamic resource allocation for mobile multihop multichannel wireless networking," in *Proc. IEEE Military Communications Conf.*, Oct. 1999, pp. 271-275.
- [34] W. Hu, H. Yousefi'zadeh, and X. Li, "Load Adaptive MAC: A Hybrid MAC Protocol for MIMO SDR MANETs," *IEEE Trans. Wireless Commun.*, vol. 10, no. 11, pp. 3924-3933, Dec. 2011.
- [35] J. Kivinen, X. Zhao, and P. Vainikainen, "Empirical characterization of wideband indoor radio channel at 5.3 Ghz," *IEEE Trans. Antennas Propag.*, vol. 49, no. 8, pp. 1192-1203, Aug. 2001.
- [36] H. Yousefi'zadeh, H. Jafarkhani, M. Moshfeghi, "Power Optimization of Wireless Media Systems with Space-Time Block Codes," *IEEE Trans. on Image Processing*, July 2004.
- [37] H. Yousefi'zadeh, H. Jafarkhani, "An Optimal Power-Throughput Trade-off Study for MIMO Fading Ad-Hoc Networks," *KICS/IEEE J. of Communications and Networks (JCN)*, Invited Paper, August 2010.
- [38] Q. Dong and W. Dargie, "A survey on mobility and mobility-aware mac protocols in wireless sensor networks," *IEEE Commun. Surveys Tuts.*, vol. 15, no. 1, pp. 88-100, Feb. 2013
- [39] D. P. Bertsekas, *Dynamic Programming and Optimal Control*. Belmont, MA: Athena Scientific, 2005.
- [40] R. A. Berry, R. G. Gallager, "Communication over fading channels with delay constraints," *IEEE Tran. on Inf. Theory*, vol. 48, no. 5, pp. 1135-1149, May 2002.
- [41] M. Zafer, E. Modiano, "Optimal adaptive data transmission over a fading channel with deadline and power constraints," in *Proc. Annu. Conf. Inform. Sci. Syst.*, 2006, pp. 931-937.
- [42] M. Zafer, B. J. Ko, I. W. -H. Ho, "Transmit power estimation using spatially diverse measurements under wireless fading," *IEEE/ACM Trans. Netw.*, vol. 18, no. 4, pp. 1171-1180, Aug. 2010.
- [43] D. Halperin, B. Greensteiny, A. Shethy, and D. Wetherall, "Demystifying 802.11n power consumption," in *Proc. 2010 Int. Conf. Power Aware Comput. and Syst.*, 2010, pp. 1-5.
- [44] D. Zwilliger, *A Handbook of Differential Equations*. New York: Academic Press, 1989, Chapter 2.
- [45] M. Zafer and E. Modiano, "A calculus approach to energy-efficient data transmission with quality-of-service constraints," *IEEE/ACM Trans. Netw.*, vol. 17, no. 3, pp. 898-911, Jun. 2009.



Siqian Cui received his B.E. degree in communication engineering from Harbin Engineering University, Harbin, China, in 2007 and his M.E. degree in information engineering from Harbin Institute of Technology, Harbin, China, in 2010. He is a Ph.D. candidate at Harbin Institute of Technology. His research interests include multi-hop wireless networks and satellite communication systems.



Homayoun Yousefi'zadeh received E.E.E and Ph.D. degrees from the Dept. of EE-Systems at USC in 1995 and 1997, respectively. Currently, he is an Adjunct Professor at the Department of EECS at UC, Irvine. In the recent past, he was a Consulting Chief Technologist at the Boeing Company and the CTO of TierFleet. He is the inventor of several US patents, has published more than seventy scholarly reviewed articles, and authored more than twenty design articles associated with deployed industry products. Dr. Yousefi'zadeh is/was with the editorial board of IEEE TRANSACTIONS ON WIRELESS COMMUNICATIONS, IEEE COMMUNICATIONS LETTERS, IEEE Wireless Communications Magazine, the lead guest editor of IEEE JSTSP for the issue of April 2008, and Journal of Communications Networks. He was the founding Chairperson of systems' management workgroup of the SNIA and a member of the scientific advisory board of Integrated Media Services Center at USC. He is a Senior Member of the IEEE and the recipient of multiple best paper, faculty, and engineering excellence awards.



communications.

Xuemai Gu received B.E., M.E., and Ph.D. degrees in communication engineering from Harbin Institute of Technology, Harbin, China, in 1982, 1985 and 1991, respectively. He is a Professor with the Communication Research Center, Harbin Institute of Technology, Harbin, China. He is the Dean of School of Electronic and Information Engineering. He is the inventor of more than 20 China patents, has published over 150 research papers. His general interests include wireless networks and transmissions, private wireless communication systems and satellite